

Aligning spins in antiferromagnetic films using antiferromagnets

S. I. Csizsar,¹ M. W. Haverkort,² T. Burnus,² Z. Hu,² A. Tanaka,³ H. H. Hsieh,⁴ H.-J. Lin,⁵ C. T. Chen,⁵ J. C. Cezar,⁶ N. B. Brookes,⁶ T. Hibma,¹ and L. H. Tjeng^{2,*}

¹*MSC, University of Groningen, Nijenborgh 4, 9747 AG Groningen, The Netherlands*

²*II. Physikalisches Institut, Universität zu Köln, Zülpicher Str. 77, 50937 Köln, Germany*

³*Department of Quantum Matter, ADSM, Hiroshima University, Higashi-Hiroshima 739-8530, Japan*

⁴*Chung Cheng Institute of Technology, National Defense University, Taoyuan 335, Taiwan*

⁵*National Synchrotron Radiation Research Center, 101 Hsin-Ann Road, Hsinchu 30077, Taiwan*

⁶*European Synchrotron Radiation Facility, BP 220, 38043, Grenoble, France*

(Dated: October 25, 2018)

We have explored the possibility to orient spins in antiferromagnetic thin films with low magnetocrystalline anisotropy via the exchange coupling to adjacent antiferromagnetic films with high magnetocrystalline anisotropy. We have used MnO as a prototype for a system with negligible single-ion anisotropy. We were able to control its spin direction very effectively by growing it as a film on antiferromagnetic CoO films with different predetermined spin orientations. This result may pave the way for tailoring antiferromagnets with low magnetocrystalline anisotropy for applications in exchange bias systems. Very detailed information concerning the exchange coupling and strain effects was obtained from the Mn $L_{2,3}$ soft x-ray absorption spectroscopy.

The study of the exchange bias phenomena in multi-layered magnetic systems is a very active research field in magnetism, not the least motivated by the high potential for applications in information technology. Various combinations of antiferromagnetic (AFM) and ferromagnetic (FM) thin film materials have been fabricated and intensively investigated.^{1,2} There seems to be an agreement among the experimental and theoretical studies that the largest exchange bias effects can be found in systems containing AFMs with a high magnetocrystalline anisotropy, such as CoO. The simple underlying idea is that the anisotropy helps to fix the spin orientation in the AFM while switching the magnetization in the FM.

Our objective is to explore the possibilities to control and to pin the spin direction in AFM oxides having low magnetocrystalline anisotropy, e.g. transition-metal oxides with the $3d^3$, $3d^5$, or $3d^8$ ionic configurations. If successful, this would help to extend the materials basis

for the AFMs used in exchange bias systems. One could then consider thin films of not only NiO but also LaCrO_3 , LaFeO_3 , $\gamma\text{-Fe}_2\text{O}_3$, and $\text{R}_3\text{Fe}_5\text{O}_{12}$.³ At first sight, our chances may seem bleak since a recent study on ultra thin NiO films reveals that the magnetic anisotropy results from a detailed balance between the influence of strain and thickness on the already very weak dipolar interactions in the AFM.^{4,5} Also a very recent detailed report on MnO thin films grown on Ag(100) substrates⁶ did not address the magnetic properties of the oxide film, suggesting that it is difficult to detect magnetic order in those films. Indeed, we ourselves have carried out at the ID08 beamline of the ESRF in Grenoble polarization dependent x-ray absorption spectroscopy (XAS) measurements at the Mn $L_{2,3}$ edges for a 50 monolayer (ML) thin film of MnO epitaxially grown on Ag(100) and, as shown in Fig.1, we could not observe any linear dichroic effect which otherwise could have unambiguously indicated the presence of antiferromagnetic order like there is for NiO on MgO.^{7,8} This is most probably the result of having several differently orientated anti-ferromagnetic domains in the sample, canceling the net linear dichroic effect.

On the other hand, the few studies available in the literature on combinations of AFM/AFM films revealed that the interlayer exchange coupling can be very strong.^{9,10,11,12,13,14,15} We took these findings as starting point of our work. We have used MnO as an ideal model for an antiferromagnetic system with negligible single-ion anisotropy. For the antiferromagnetic material with strong single-ion anisotropy we chose CoO. We note that large magnetization loops shifts have been reported for MnO nanocrystallites deposited by reactive ion beam on Co metal,¹⁶ which we took as support for our hypothesis that CoO/MnO interfaces may play an important role for the magnetic coupling. We have grown MnO as a thin film epitaxially on two different types of CoO single crystal films. In one CoO film the spin direction is oriented perpendicular to the surface, and in the other parallel to

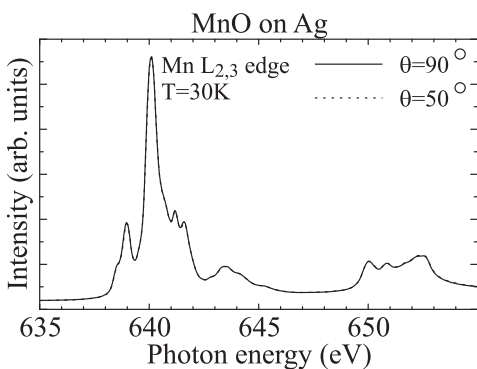


FIG. 1: Mn $L_{2,3}$ XAS spectra of a 50 monolayer MnO film epitaxially grown in Ag(001). The spectra were taken with linearly polarized light, in which θ is the angle between the electric field vector \vec{E} and the [001] surface normal. The sample was measured at 30 K.

the surface.¹⁷ Using soft x-ray absorption spectroscopy at the Mn $L_{2,3}$ edges, we will show below that the spin direction of the MnO film strongly depends on the type of CoO film the MnO is grown on, and that it is dictated by the spin orientation of the CoO film and not by the strain or dipolar interactions in the MnO film. Interlayer exchange coupling is thus a very effective manner to control spin directions and may be used for tailoring AFMs with low magnetocrystalline anisotropy for exchange bias applications.

The actual MnO/CoO systems studied are (14Å)MnO/(10Å)CoO/(100Å)MnO/Ag(001) and (22Å)MnO/(90Å)CoO/Ag(001). The two samples were grown on a Ag(001) single crystal by molecular beam epitaxy (MBE), evaporating elemental Mn and Co from alumina crucibles in a pure oxygen atmosphere of 10^{-7} to 10^{-6} mbar. The base pressure of the MBE system is in the low 10^{-10} mbar range. The thickness and epitaxial quality of the films are monitored by reflection high energy electron diffraction (RHEED) measurements. Both the CoO and MnO films had [001]/[001] epitaxial relationships with the underlying Ag(001) substrate. With the lattice constants of bulk Ag, CoO, and MnO being 4.09Å, 4.26Å, and 4.444Å, respectively, we find from x-ray diffraction (XRD) and RHEED that the in-plane lattice constants in each film are essentially given by the thickest layer which is almost bulk like. Compared to the bulk, the 10Å CoO sandwiched by MnO is about 4% expanded in-plane ($a_{||} \approx 4.424\text{\AA}$), while the 90Å CoO directly on Ag is slightly compressed in-plane ($a_{||} \approx 4.235\text{\AA}$, $a_{\perp} \approx 4.285\text{\AA}$). The MnO is compressed in both samples, but much more so for the one on the 90Å CoO film. Details about the growth is given elsewhere.¹⁸ We have recently shown that the spin direction is oriented perpendicular to the surface in the CoO film under tensile in-plane stress, and that it is parallel to the surface in the film with the slightly compressive in-plane stress.¹⁷

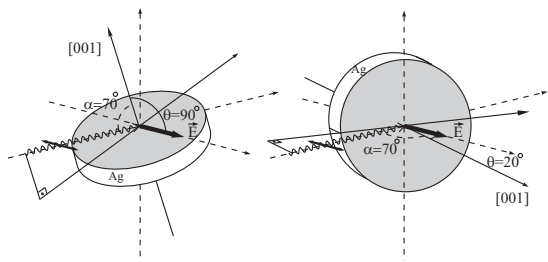


FIG. 2: Experimental XAS geometry, with polarization of the light in the horizontal plane. θ is the angle between the electric field vector \vec{E} and the [001] surface normal, and α the tilt between the Poynting vector and the surface normal.

The XAS measurements were performed at the Dragon beamline of the NSRRC in Taiwan using *in-situ* MBE grown samples. The spectra were recorded using the total electron yield method in a chamber with a base pressure of 3×10^{-10} mbar. The photon energy resolution at

the Mn $L_{2,3}$ edges ($h\nu \approx 635 - 655$ eV) was set at 0.2 eV, and the degree of linear polarization was $\approx 98\%$. The sample was tilted with respect to the incoming beam, so that the Poynting vector of the light makes an angle of $\alpha = 70^\circ$ with respect to the [001] surface normal. To change the polarization, the sample was rotated around the Poynting vector axis as depicted in Fig. 2, so that θ , the angle between the electric field vector \vec{E} and the [001] surface normal, can be varied between 20° and 90° . This measurement geometry allows for an optical path of the incoming beam which is independent of θ , guaranteeing a reliable comparison of the spectral line shapes as a function of θ . A MnO single crystal is measured *simultaneously* in a separate chamber to obtain a relative energy reference with an accuracy of better than 0.02 eV.

Fig. 3 shows the polarization dependent Mn $L_{2,3}$ XAS spectra of the MnO/CoO samples with CoO spin-orientation perpendicular (left panel) and parallel (right panel) to the surface, taken at temperatures far below (top part) and far above (bottom part) the Néel temperature (T_N) of the MnO thin film, which is about 130 K as we will show below. The spectra have been corrected for electron yield saturation effects.¹⁹ The general line shape of the spectra shows the characteristic features of bulk MnO,²⁰ demonstrating the good quality of our MnO films. Very striking in the spectra is the clear polarization dependence, which is the strongest at low temperatures. It is important to note that below T_N the dichroism, i.e. the polarization dependence, of the two samples are opposite: for instance, the intensity of the peak A at $h\nu = 639$ eV is higher for $\theta = 20^\circ$ than for $\theta = 90^\circ$ in MnO/CoO where the spin orientation of the CoO is out of plane, while it is smaller in the other sample. Above T_N , the dichroism almost vanishes. Nevertheless, small but clear and reproducible shifts in the spectra as a function of polarization can be seen: peak B at 640 eV has a shift of about 30 meV for the MnO sandwiching the 10Å CoO film, and 150 meV for the MnO grown on top of the 90Å CoO film.

In order to resolve the origin of the dichroism in the spectra, we have investigated the temperature dependence in more detail. The measurements were done by taking the spectra starting from the lowest temperature ($T=67\text{K}$ or $T=77\text{K}$) towards higher temperatures and after the highest temperature was reached ($T=200\text{K}$ or $T=400\text{K}$) we returned to low temperatures and acquired new spectra in between the previously measured temperatures. Fig. 4 depicts the polarization contrast of peak A , defined as the difference divided by the sum of the peak height in the spectra taken with the $\theta = 20^\circ$ and $\theta = 90^\circ$ polarizations. In going from low to high temperatures, one can see a significant temperature dependence for both samples (with opposite signs), which flattens off at about 130K, identified as the T_N of these MnO thin films. We therefore infer that at low temperatures the strong dichroic signal is caused by the presence of magnetic ordering. Important is to note that the opposite sign in the dichroism for the two samples implies that

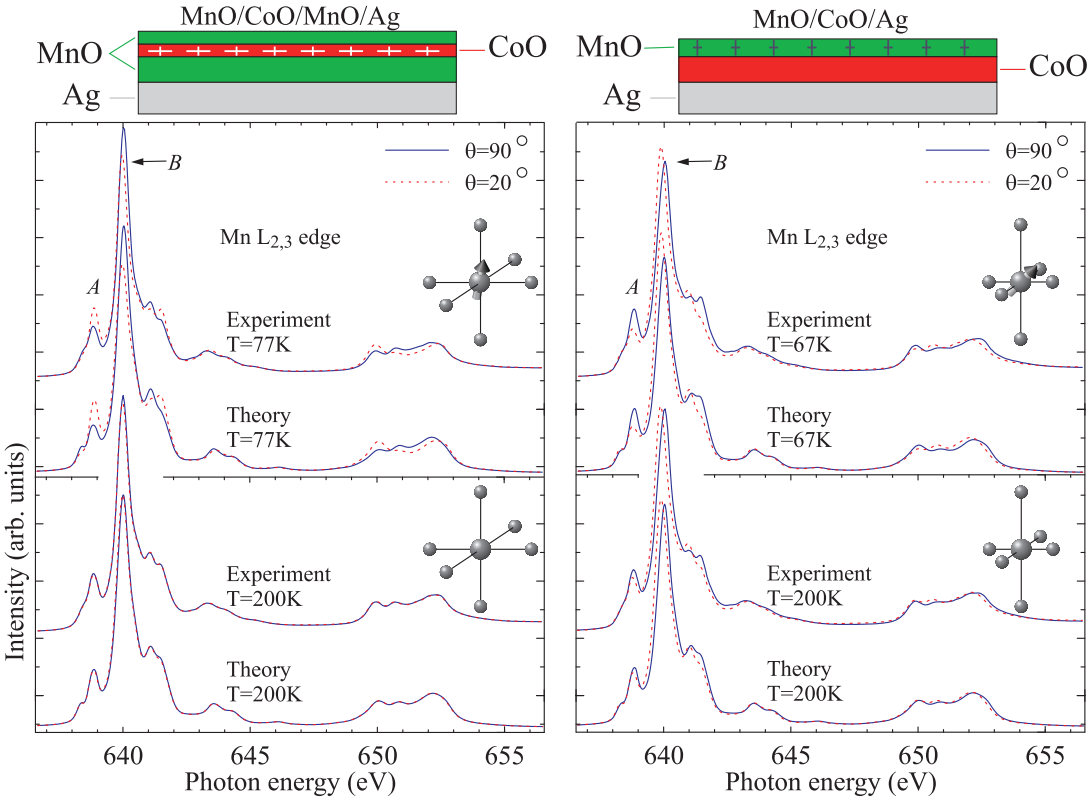


FIG. 3: (color online) Experimental and calculated Mn $L_{2,3}$ XAS spectra of MnO in (left panel) (14 Å)MnO/(10 Å)CoO/(100 Å)MnO/Ag(001) and (right panel) (22 Å)MnO/(90 Å)CoO/Ag(001) for $\theta = 20^\circ$ and $\theta = 90^\circ$. Spectra below (T=77K left, T=67K right panel) and above (T=200K) the T_N of the MnO film are shown in the top and bottom parts, respectively.

the orientation of the magnetic moments is quite different. Here we recall that MnO films grown on Ag *without* CoO do not show any dichroism down to the lowest temperatures, indicating the crucial role of the CoO in orienting the magnetic moments of the MnO.

To understand the Mn $L_{2,3}$ spectra quantitatively, we performed calculations for the atomic-like $2p^63d^5 \rightarrow 2p^53d^6$ transitions using a similar method as described by Kuiper *et al.*²¹ and Alders *et al.*,⁸ but now in a D_{4h} point group symmetry and including covalency. The method uses a MnO₆ cluster which includes the full atomic multiplet theory and the local effects of the solid.^{20,23} It accounts for the intra-atomic 3d-3d and 2p-3d Coulomb and exchange interactions, the atomic 2p and 3d spin-orbit couplings, the O 2p - Mn 3d hybridization, local crystal field parameters $10Dq$, D_s , and D_t , and a Brillouin-type temperature dependent exchange field which acts on spins only and vanishes at T_N . As in earlier works,^{8,17} an average has been made over all possible equivalent magnetic domains in the local D_{4h} crystal-field point group, canceling out the effects of anisotropic magnetic linear dichroism.²² The calculations were carried out using the XTLS 8.0 program.²³

The results of the calculations are shown in Fig. 3. We used the parameters already known for bulk MnO,^{23,24} and tuned only the parameters for D_s , D_t , and the di-

rection of the exchange field. For the MnO sandwiching the 10 Å CoO we find an excellent simulation of the experimental spectra for $D_s = 9.3$ meV, $D_t = 2.6$ meV, and an exchange field parallel to the [112] direction. For the MnO overlaying the 90 Å CoO we obtained the best fit for $D_s = 48.6$ meV, $D_t = 11.1$ meV, and an exchange field along the [211] direction. These two sets of parameters reproduce the spectra at all temperatures extremely well. This is also demonstrated in Fig. 4, showing the excellent agreement between the calculated and measured temperature dependence of the dichroism in peak A. Most important is obviously the information concerning the spin direction that can be extracted from these simulations. Earlier results have shown that in-plane tensile strained CoO layers ($c/a < 1$) have their spin orientation parallel with the [001] direction while slightly compressed CoO/Ag(001) layers ($c/a > 1$) have spin orientation perpendicular with the [001] direction.¹⁷ We thus find that the magnetic moments in the MnO are oriented towards the surface normal when it is grown on the CoO film which has the spin direction perpendicular to the surface, and that it is lying towards the surface when MnO is grown on the CoO film which has the parallel alignment. In other words, it seems that bulk-like MnO domains are stabilized that follow the CoO spin-

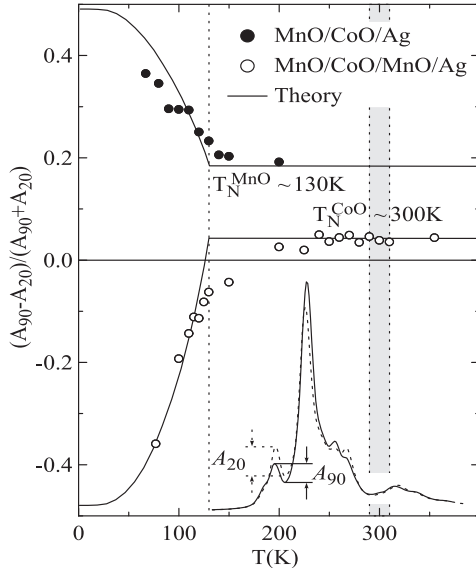


FIG. 4: Temperature dependence of the polarization contrast in the Mn $L_{2,3}$ spectra, defined as the difference divided by the sum of the height of peak A at $h\nu = 639$ eV, taken with $\theta = 20^\circ$ and $\theta = 90^\circ$ polarizations. Filled and empty circles are the experimental data. The solid lines are the theoretical simulations. The shaded area represents the T_N of the CoO layers under the MnO film.

direction as much as possible.

In order to find out whether the spin direction in the MnO thin films is determined by the exchange coupling with the CoO, or whether it is given by strain and dipole interactions in the films as found for NiO thin films on non-magnetic substrates,^{4,5} we now have to look more closely into the tetragonal crystal fields in the MnO films. The values for the tetragonal crystal field parameters D_s and D_t , which we have used to obtain the excellent simulations as plotted in Fig. 3, can actually be extracted almost directly from the high-temperature spectra, where the magnetic order has vanished and does not contribute anymore to the polarization dependence.

The top panels of Fig. 5 show a close-up of the spectra taken at 200K, i.e. above T_N . One can now observe the small but clear and reproducible shifts in the spectra as a function of polarization: the shift in peak A is denoted by Δ_A and in peak B by Δ_B . In order to understand intuitively the origin of these shifts, we will start to describe the energetics of the high spin Mn^{2+} ($3d^5$) ion in a one-electron-like picture. In O_h symmetry the atomic $3d$ levels are split into $3 t_{2g}$ and $2 e_g$ orbitals, all containing a spin-up electron. The L_3 edge of Mn^{2+} should then consist of two peaks: in exciting an electron from the $2p$ core level to the $3d$, one can add an extra spin-down electron either to the lower lying t_{2g} or the higher lying e_g shell, producing peaks A and B , respectively. In the presence of a tetragonal distortion, both the t_{2g} and e_g levels will be split, resulting in a polarization dependent shifts Δ_A and Δ_B , analogous as found for NiO.²⁵

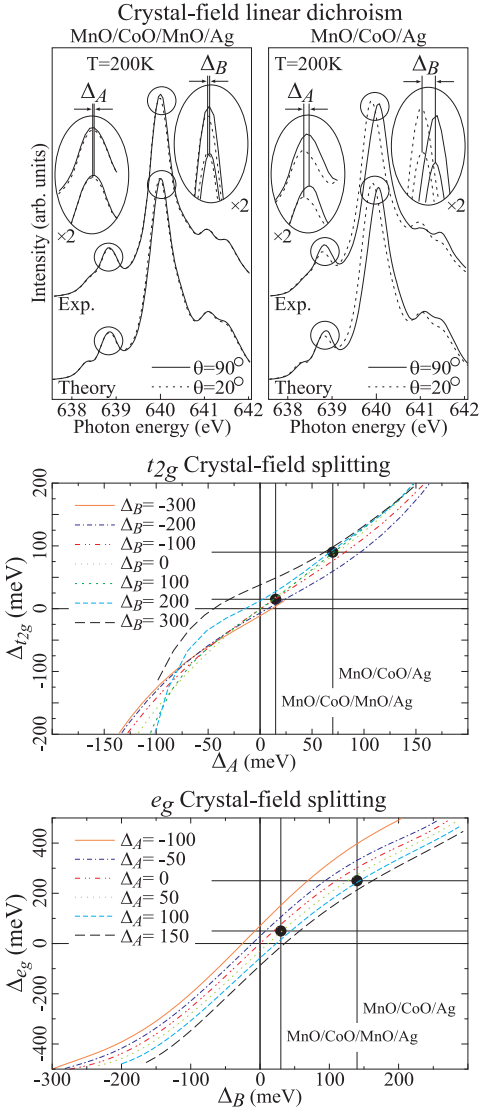


FIG. 5: (color online) (top panel) Close-up of the experimental and calculated Mn L_3 XAS spectra at 200K, i.e. above T_N of (left) (14 Å)MnO/(10 Å)CoO/(100 Å)MnO/Ag(001) and (right) (22 Å)MnO/(90 Å)CoO/Ag(001); Δ_A and Δ_B are the polarization dependent shifts in peaks A and B , respectively; (middle and bottom panels) Relationship between $\{\Delta_A, \Delta_B\}$ and the tetragonal $\{\Delta_{t_{2g}}, \Delta_{e_g}\}$ splittings.

Due to the intra-atomic $2p$ - $3d$ and $3d$ - $3d$ electron correlation effects, the relationship between the shifts in the spectra and the crystal field splittings become non-linear. Using the cluster model we are able to calculate this relationship for a Mn^{2+} $3d^5$ system and the results are plotted in Fig. 5. Using this map, we find for the MnO sandwiching the 10 Å CoO that $\Delta_{t_{2g}} = 15$ meV and $\Delta_{e_g} = 50$ meV, and for the MnO overlaying the 90 Å CoO that $\Delta_{t_{2g}} = 90$ meV and $\Delta_{e_g} = 250$ meV ($D_s = (\Delta_{e_g} + \Delta_{t_{2g}})/7$, $D_t = (3\Delta_{e_g} - 4\Delta_{t_{2g}})/35$). The crystal field splittings for the second sample are much larger than for the first sample. This is fully consistent with

our structural data which indicate that in the second sample MnO experiences a much stronger compressive in-plane strain. It is important to recognize that the crystal field splittings for the two samples have the same sign, i.e. that both MnO films are compressed in plane. This implies that strain together with the dipolar interactions cannot explain the quite different spin-orientations of the two MnO systems. We conclude that the magnetic anisotropy mechanism present in, for instance, NiO thin films on non-magnetic substrates,^{4,5} is overruled by the stronger interlayer exchange coupling^{9,10,11,12,13,14,15} between the CoO and MnO layers.

The T_N for these thin MnO layers is found to be at about 130 K. It is surprising that the Néel temperature is not reduced as compared to the bulk value of 121 K,²⁶ since generally one would expect this to happen with decreasing thickness as was observed for NiO on MgO.⁸ The origin for such a surprising behavior is not clear at this moment. It is possible that the in-plane compressive stress causes an increase in the Mn 3d - O 2p hybridization, which in turn could produce an increase of the superexchange interaction strength³ and thus also of T_N . Another, more exciting, possibility emerges from the recent experimental

and theoretical work on AFM/AFM multilayers such as FeF₂/CoF₂ and CoO/NiO.^{9,10,11,12,13,14,15} Experiments have revealed that multilayers could even have a single magnetic ordering transition temperature lying in between the two T_N s of the constituent materials. The phenomenon has been ascribed to the very strong interlayer exchange coupling.

In conclusion, we have shown that it is possible to control the spin direction in MnO very effectively by growing them as thin films on antiferromagnetic CoO films with different predetermined spin orientations. Using detailed Mn $L_{2,3}$ soft x-ray absorption spectroscopy, we are also able to show that it is not strain but interlayer exchange coupling which plays a decisive role herein. This result may pave the way for tailoring antiferromagnets with low magnetocrystalline anisotropy for applications in exchange bias.

We acknowledge the NSRRC and ESRF staff for providing us with an extremely stable beam. We would like to thank Lucie Hamdan and Henk Bruinenberg for their skillful technical and organizational assistance in preparing the experiment. The research in Cologne is supported by the Deutsche Forschungsgemeinschaft through SFB 608.

* Corresponding author: tjeng@ph2.uni-koeln.de

¹ See for review: J. Nogués and I. K. Schuller, *J. Magn. Magn. Mater.* **192**, 203 (1999).

² See for review: A. E. Berkowitz and K. Takano, *J. Magn. Magn. Mater.* **200**, 552 (1999).

³ J. B. Goodenough, *Magnetism and the Chemical Bond* (Wiley, New York, 1963).

⁴ S. Altieri, M. Finazzi, H. H. Hsieh, H.-J. Lin, C. T. Chen, T. Hibma, S. Valeri, and G. A. Sawatzky, *Phys. Rev. Lett.* **91**, 137201 (2003).

⁵ M. Finazzi and S. Altieri, *Phys. Rev. B* **68**, 054420 (2003).

⁶ M. Nagel, I. Biswas, P. Nagel, E. Pellegrin, S. Schuppler, H. Peisert, and T. Chassé, *Phys. Rev. B* **75**, 195426 (2007).

⁷ D. Alders, J. Vogel, C. Levelut, S. D. Peacor, T. Hibma, M. Sacchi, L. H. Tjeng, C. T. Chen, G. van der Laan, B. T. Thole, and G. A. Sawatzky, *Europhys. Lett.* **32**, 259 (1995).

⁸ D. Alders, L. H. Tjeng, F. C. Voogt, T. Hibma, G. A. Sawatzky, J. Vogel, M. Sacchi, S. Iacobucci, and C. T. Chen, *Phys. Rev. B* **57**, 11623 (1998).

⁹ C. A. Ramos, D. Lederman, A. R. King, and V. Jaccarino, *Phys. Rev. Lett.* **65**, 2913 (1990).

¹⁰ A. S. Carriço and R. E. Camley, *Phys. Rev. B* **45**, 13117 (1992).

¹¹ R. W. Wang and D. L. Mills, *Phys. Rev. B* **46**, 11681 (1992).

¹² D. Lederman, C. A. Ramos and V. Jaccarino, and J. L. Cardy, *Phys. Rev. B*, **48**, 8365 (1993).

¹³ J. A. Borchers, M. J. Carey, R. W. Erwin, C. F. Majkrzak, and A. E. Berkowitz, *Phys. Rev. Lett.* **70**, 1878 (1993).

¹⁴ M. J. Carey, A. E. Berkowitz, J. A. Borchers, and R. W.

Erwin, *Phys. Rev. B* **47**, 9952 (1993).

¹⁵ E. N. Abarra, K. Takano, F. Hellman, and A. E. Berkowitz, *Phys. Rev. Lett.* **77**, 3451 (1996).

¹⁶ J. van Lierop, M. A. Schofield, L. H. Lewis, R. J. Gambino, *J. Magn. Magn. Mater.* **264**, 146 (2003).

¹⁷ S. I. Csiszar, M. W. Haverkort, Z. Hu, A. Tanaka, H. H. Hsieh, H.-J. Lin, C. T. Chen, T. Hibma, and L. H. Tjeng, *Phys. Rev. Lett.* **95**, 187205 (2005).

¹⁸ S. I. Csiszar, thesis, University of Groningen (2005); <http://irs.ub.rug.nl/ppn/287545644>.

¹⁹ R. Nakajima, J. Stöhr and Y. U. Idzerda, *Phys. Rev. B*, **59**, 6421 (1999).

²⁰ See review by F. M. F. de Groot, *J. Electron Spectrosc. Relat. Phenom.* **67**, 529 (1994).

²¹ P. Kuiper, B. G. Searle, P. Rudolf, L. H. Tjeng, and C. T. Chen, *Phys. Rev. Lett.* **70**, 1549 (1993).

²² E. Arenholz, G. van der Laan, R. V. Chopdekar, and Y. Suzuki, *Phys. Rev. B* **74**, 094407 (2006).

²³ A. Tanaka and T. Jo, *J. Phys. Soc. Jpn.* **63**, 2788 (1994).

²⁴ Parameters for MnO₆ cluster [eV]: $\Delta=8.0$, $U_{dd}=5.5$, $U_{cd}=7.2$, $V_{eg}=-2.1$, $T_{pp}=0.7$, $10Dq=0.5+70/12 Dt$, $\zeta=0.066$, $H_{ex}=0.0135$; Slater integrals 80% of Hartree-Fock values; MnO/CoO/MnO/Ag(100): $Ds=0.0093$, $Dt=0.0026$; MnO/CoO/Ag(100): $Ds=0.0486$, $Dt=0.0111$. H_{ex} from G. Pepy, *J. Phys. Chem. Solids* **35**, 433 (1974).

²⁵ M. W. Haverkort, S. I. Csiszar, Z. Hu, S. Altieri, A. Tanaka, H. H. Hsieh, H.-J. Lin, C. T. Chen, T. Hibma, and L. H. Tjeng, *Phys. Rev. B* **69**, 020408 (2004)

²⁶ C. G. Shull, W. A. Strauser, E. O. Wollan, *Phys. Rev.* **83**, 333 (1951).